Alpha particles diffusion due to charge changes

Cite as: Phys. Plasmas **22**, 122502 (2015); https://doi.org/10.1063/1.4936875
Submitted: 29 September 2015 • Accepted: 18 November 2015 • Published Online: 07 December 2015

C. F. Clauser and R. Farengo

Alpha particles diffusion due to charge changes

C. F. Clauser[a] and R. Farengo
Centro Atómico Bariloche and Instituto Balseiro, Comisión Nacional de Energía Atómica and Universidad Nacional de Cuyo, Av. Bustillo 9500, 8400 Bariloche, Argentina

(Received 29 September 2015; accepted 18 November 2015; published online 7 December 2015)

Alpha particles diffusion due to charge changes in a magnetized plasma is studied. Analytical calculations and numerical simulations are employed to show that this process can be very important in the pedestal-edge-SOL regions. This is the first study that presents clear evidence of the importance of atomic processes on the diffusion of alpha particles. A simple 1D model that includes inelastic collisions with plasma species, "cold" neutrals, and partially ionized species was employed. The code, which follows the exact particle orbits and includes the effect of inelastic collisions via a Monte Carlo type random process, runs on a graphic processor unit (GPU). The analytical and numerical results show excellent agreement when a uniform background (plasma and cold species) is assumed. The simulations also show that the gradients in the density of the plasma and cold species, which are large and opposite in the edge region, produce an inward flux of alpha particles. Calculations of the alpha particles flux reaching the walls or divertor plates should include these processes. © *2015 AIP Publishing LLC*. [http://dx.doi.org/10.1063/1.4936875]

I. INTRODUCTION

The alpha particles produced in D-T reactions will play a critical role in fusion reactors. The power deposited by these particles will be the main heating source available to compensate the losses and keep the plasma temperature constant. Any process that affects the confinement of high energy alpha particles can therefore reduce the performance of the reactor. On the other hand, the removal of low energy alpha particles (helium ash) is needed to avoid the dilution of the fuel and sustain a high fusion power. While Coulomb collisions produce an unavoidable particle diffusion, other ("anomalous") processes can result in significantly higher diffusion rates. These include large scale MHD fluctuations, Alfvèn eigenmodes, microturbulence, toroidal ripple, and perturbations produced by ELM control coils.

We show here that inelastic collisions that change the charge state of the alpha particles, and therefore their Larmor radius, can also produce significant diffusion. We will call this process "inelastic diffusion." Inelastic diffusion was first studied by Fussmann[1] who derived analytic expressions for the diffusion coefficient resulting from charge changes. When these equations are applied to alpha particles confined in the core of the reactor and subjected only to radiative recombination (RR) processes the resulting diffusion coefficient is negligible. In the pedestal-edge-scrape-off layer (SOL) region, however, the density of neutral atoms and impurities will be high enough for other charge changing processes to become important.

We use a simple 1D model and particle simulations to show that for realistic parameters a large diffusion coefficient is obtained in the pedestal-edge-SOL region. The accurate calculation of the alpha particles flux and power reaching the wall and divertor plates is very important to guarantee a safe reactor operation and various studies have been performed recently.[2,3] Our results indicate that these calculations should include inelastic collisions to obtain realistic results.

The structure of this paper is the following. In Sec. II, we discuss the basic physics of the diffusion produced by charge changes and present analytic expressions for the diffusion coefficient. In Sec. III, the charge changing processes considered and their reaction rates are introduced. Sec. IV contains the results of analytical calculations and particle simulation and Sec. V, the summary and conclusions.

II. INELASTIC DIFFUSION

As we mentioned in Section I, inelastic diffusion occurs when the charge of a particle changes. This produces a change in the Larmor radius and results in a jump in the position of its guiding center. Furthermore, if the particle becomes neutral it will move in a straight line, thus increasing the magnitude of the displacement. To illustrate this mechanism, we show, in Fig. 1, how charge changes can produce a diffusion process. In the figure, a particle rotating around a uniform magnetic field interacts with a uniform background of thermal and cold species. This interaction produces changes in the charge of the particle and "jumps" in the position of the guiding center, from "0" to "1," then "2," etc.

To describe this process, we repeat for convenience some results obtained by Fussmann.[1] The standard expression employed to calculate the particle diffusion coefficient is

$$D_\perp = \frac{1}{2}\langle \Delta l^2 \rangle_\perp \nu, \tag{1}$$

where Δl is the particle displacement due to the process considered, ν is the frequency, and $\langle\rangle$ means ensemble average. The subscript $\perp$ refers to the fact that the diffusion is

[a]Electronic mail: cesar.clauser@ib.edu.ar

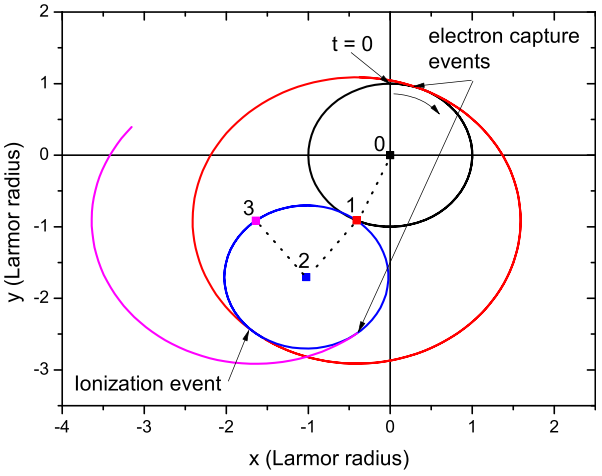

FIG. 1. Inelastic diffusion example. When a particle changes its charge, the change in its Larmor radius produces a jump in the guiding center position.

perpendicular to the magnetic field, but in the following we will omit this label. It is useful to split up the diffusion coefficient as the sum of various contributions,

$$D = \sum_{Z=1}^{Z_N} D_Z.$$

Here, D_Z is defined as the diffusion coefficient for charge changes between Z and $Z-1$. Thus,

$$D_Z = \frac{1}{2}\langle \Delta l^2_{Z\to Z-1}\rangle f_Z \nu_{Z\to Z-1} + \frac{1}{2}\langle \Delta l^2_{Z-1\to Z}\rangle f_{Z-1}\nu_{Z-1\to Z}, \quad (2)$$

where $f_Z = n_{\alpha,Z}/n_\alpha$ is the fraction of particles in a given charge state and $\nu_{Z\to Z\pm1}$ is the collision frequency. The latter is the typical frequency for charge changes from Z to $Z\pm1$ due to atomic processes (see Section II A). As a general rule,

$$\frac{df_Z}{dt} = -f_Z(\nu_{Z\to Z-1} + \nu_{Z\to Z+1}) + f_{Z-1}\nu_{Z-1\to Z} + f_{Z+1}\nu_{Z+1\to Z}.$$

In the following, we assume that these fractions are in equilibrium ($df/dt = 0$) and use this condition to calculate the fraction of particles in each charge state.

A. Diffusion without neutral state

Let us consider, as the first example, alpha particles which cannot be neutralized. In this case, $D = D_2$ and the equilibrium condition gives

$$f_2 = \frac{\nu_{1\to2}}{\nu_{1\to2} + \nu_{2\to1}}$$

and

$$f_1 = \frac{\nu_{2\to1}}{\nu_{1\to2} + \nu_{2\to1}},$$

where the condition $f_1 + f_2 = 1$ has been used. Moreover, $\Delta l = \Delta\rho$ is the change in Larmor radius due to the charge change

$$\Delta\rho_{Z\to Z\pm1} = \frac{v_\perp}{\Omega_Z}\frac{1}{Z\pm1}, \quad (3)$$

where Ω_Z is the gyro-frequency of a projectile with charge Z and $v_\perp$ its perpendicular velocity. Then

$$D = \frac{\langle v_\perp^2\rangle}{\Omega_2^2}\nu. \quad (4)$$

In Eq. (4), ν is an effective collision frequency for the process

$$\nu = \frac{\nu_{2\to1}\nu_{1\to2}}{\nu_{2\to1} + \nu_{1\to2}}. \quad (5)$$

We can consider two limits; if $\nu_{1\to2} \gg \nu_{2\to1}$ the effective collision frequency reduces to

$$\nu \to \nu_{2\to1}. \quad (6)$$

On the other hand, if $\nu_{2\to1} \gg \nu_{1\to2}$ Eq. (5) reduces to

$$\nu \to \nu_{1\to2}. \quad (7)$$

Hence, in this case, the effective collision frequency is limited by the process with the lowest collision frequency.

B. Diffusion with neutral state

As a second example, we consider the general case in which alpha particles can be neutralized. In this case,

$$D = D_2 + D_1, \quad (8)$$

and, in equilibrium, we have

$$f_2 = \frac{\nu_{0\to1}\nu_{1\to2}}{\nu_{2\to1}\nu_{1\to0} + \nu_{2\to1}\nu_{0\to1} + \nu_{0\to1}\nu_{1\to2}},$$
$$f_1 = \frac{\nu_{2\to1}\nu_{0\to1}}{\nu_{2\to1}\nu_{1\to0} + \nu_{2\to1}\nu_{0\to1} + \nu_{0\to1}\nu_{1\to2}},$$
$$f_0 = \frac{\nu_{2\to1}\nu_{1\to0}}{\nu_{2\to1}\nu_{1\to0} + \nu_{2\to1}\nu_{0\to1} + \nu_{0\to1}\nu_{1\to2}}.$$

Since D_2 involves only ionized species the displacement, Δl, is given by Eq. (3),

$$D_2 = \frac{\langle v_\perp^2\rangle}{\Omega_2^2} f_1 \nu_{1\to2}. \quad (9)$$

Using Eq. (2) we can write D_1 as

$$D_1 = \frac{1}{2}\langle \Delta l^2_{1\to0}\rangle f_1\nu_{1\to0} + \frac{1}{2}\langle \Delta l^2_{0\to1}\rangle f_0\nu_{0\to1}, \quad (10)$$

where $\Delta l_{1\to0}$ is the distance traveled from the time the particle is neutralized until it becomes ionized again. It is easy to show that[1]

$$\langle \Delta l^2_{1\to0}\rangle = \langle v_\perp^2\rangle \frac{2}{\nu^2_{0\to1}}.$$

In the second term of the RHS of Eq. (10) $\Delta l_{0\to1}$ represents the distance traveled after an ionization, which is the Larmor radius. Since $\Omega_1 \gg \nu_{0\to1}$, we can approximate

$$D_1 = \frac{\langle v_\perp^2 \rangle}{\nu_{0\to1}^2} f_1 \nu_{1\to0}.$$

Finally, we have

$$D = \langle v_\perp^2 \rangle \left(\frac{\nu_{1\to2}}{\Omega_2^2} + \frac{\nu_{1\to0}}{\nu_{0\to1}^2} \right) f_1. \tag{11}$$

Equation (11) shows that the diffusion coefficient depends on the energy and pitch angle of the alpha particles ($v_\perp$), on the magnetic field and on the frequency of the processes that produce changes in the charge state. In very general plasma conditions, one can assume that ionization frequencies are much greater than recombination frequencies. In this case, we may approximate $f_1 \approx \nu_{2\to1}/\nu_{1\to2}$, and Eq. (11) reduces to

$$D \approx \langle v_\perp^2 \rangle \left(\frac{\nu_{2\to1}}{\Omega_2^2} + \frac{\nu_{2\to1}\nu_{1\to0}}{\nu_{0\to1}^2 \nu_{1\to2}} \right).$$

We can observe that the first term in the right-hand side corresponds to Eq. (4) with ν given by Eq. (7), as we expected. However, the most important term is the second, since the gyro-frequency is much larger than any collision frequency. Hence, the diffusion coefficient is very sensitive to the neutral channel.

III. ATOMIC PROCESSES

Atomic physics processes are very important in the edge and SOL regions of fusion plasmas.[4] We include several processes that involve the interaction of alpha particles with plasma species, He^+ and neutral deuterium (both atomic and molecular) and helium. We also assume that all the plasma ions are D (no T). Other possible processes are omitted because they have a much lower reaction frequency. Impurities, such as Be, W, and C, were not included because the data available are limited or have not been calculated[5] in the whole alpha particle energy range. It is clear that more and better data are needed to properly account for all the relevant processes.

As we mentioned, the processes considered include interactions with plasma (thermal) targets as well as with "cold" targets. Here, we use "cold" to refer to neutral species or partially ionized species with temperatures that are much lower than the energy of the alphas. We classified these processes in two groups. The first one, Eq. (12), includes electron capture processes (CX), which tend to reduce the charge of the alpha particles or neutralize them,

$$\begin{aligned}
\alpha^{+2} + D^0 &\to \alpha^+ + D^+ \\
\alpha^{+2} + D_2^0 &\to \alpha^+ + D_2^+ \\
\alpha^{+2} + He^0 &\to \alpha^+ + He^+ \\
\alpha^{+2} + He^+ &\to \alpha^+ + He^{+2},
\end{aligned} \tag{12a}$$

$$\begin{aligned}
\alpha^{+} + D^0 &\to \alpha^0 + D^+ \\
\alpha^{+} + D_2^0 &\to \alpha^0 + D_2^+ \\
\alpha^{+} + He^0 &\to \alpha^0 + He^+ \\
\alpha^{+} + He^+ &\to \alpha^0 + He^{+2}.
\end{aligned} \tag{12b}$$

Reactions involving the exchange of two electrons (i.e., $\alpha^{+2} + He^0 \to \alpha^0 + He^{+2}$) were not included because their reaction rates are much lower. In the second group, Eq. (13), we have electron impact ionization (EII) and electron removal (ER: DII + CX) by deuterons as well as electron capture processes, which tend to increase the charge of the alpha particles

$$\begin{aligned}
\alpha^+ + e^- &\to \alpha^{+2} + e^- + e^- \\
\alpha^+ + D^+ &\to \alpha^{+2} + D^0 \\
&\to \alpha^{+2} + D^+ + e^- \\
\alpha^+ + He^+ &\to \alpha^{+2} + He^0,
\end{aligned} \tag{13a}$$

$$\begin{aligned}
\alpha^0 + e^- &\to \alpha^+ + e^- + e^- \\
\alpha^0 + D^+ &\to \alpha^+ + D^0 \\
&\to \alpha^+ + D^+ + e^- \\
\alpha^0 + D_2^0 &\to \alpha^+ + D_2^0 + e^- \\
\alpha^0 + He^+ &\to \alpha^+ + He^0.
\end{aligned} \tag{13b}$$

To avoid confusion, we distinguish between energetic alpha particles, α, and "cold" He, which comes from the outside region.

The cross sections, σ, of all these processes are listed in the ALADDIN database.[5,6] As we mentioned before, for a projectile particle, α, the magnitude that defines if a process is important is the collision frequency $\nu_{Z\to Z\pm1}$. Furthermore, $\nu_{Z\to Z\pm1}$ involves the sum of all processes, $\nu_{\alpha\lambda}$, where λ refers to the target specie, that changes the charge from Z to $Z\pm1$. In terms of the cross section: $\nu_{\alpha\lambda} = n_\lambda \langle \sigma v \rangle_{\alpha\lambda}$. Here, n_λ is the density of the target species and $\langle \sigma v \rangle_{\alpha\lambda}$ is the corresponding reaction rate for such process. For a beam-cold target incidence, we have simply

$$\langle \sigma v \rangle_{\alpha\lambda} = \sigma v_\alpha, \tag{14}$$

where v_α is the particle velocity. For beam-Maxwellian incidence, we have

$$\langle \sigma v \rangle_{\alpha\lambda} = \left(\frac{\beta_\lambda}{\pi} \right)^{1/2} \frac{1}{v_\alpha} \int_0^\infty dv_r v_r^2 \sigma(v_r) \left[e^{-\beta_\lambda (v_\alpha - v_r)^2} - e^{-\beta_\lambda (v_\alpha + v_r)^2} \right], \tag{15}$$

where $\beta_\lambda = m_\lambda/(2T_\lambda)$ and $v_r = |\vec{v}_\alpha - \vec{v}_\lambda|$ is the relative velocity. In the definition of β_λ, m_λ is the target mass and the temperature, T_λ, is given in energy units. Eq. (14) was used for collisions with cold targets while Eq. (15) was employed for collisions with plasma species. In order to illustrate the relevance of the processes listed above, we show in Figs. 2 and 3, the reaction rates as a function of the projectile energy for those shown in Eqs. (12) and (13), respectively.

For collisions with plasma particles two temperatures are considered. The 4 keV case is representative of the conditions at the pedestal region, while the 170 eV case is representative at the edge/scrape-off layer region.

IV. RESULTS

As we mentioned above, the first one to study inelastic diffusion was Fussmann.[1] For alpha particles, he focused on

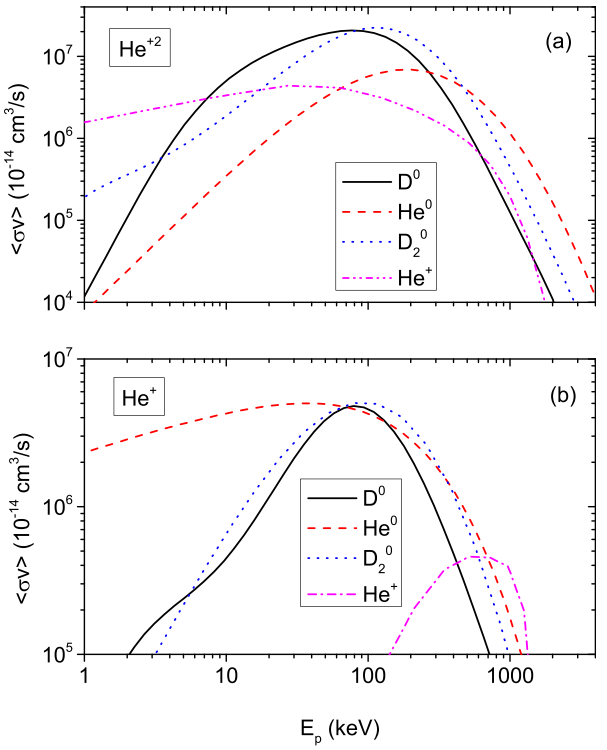

FIG. 2. Reaction rates employed for charge exchange (CX) of alpha particles with cold targets. In (a), we show the processes given by Eq. (12a) while in (b) those given by Eq. (12b).

the plasma core and only considered charge changes produced by RR. In addition, he did not include the possibility of neutralization. The collision frequency for RR can be calculated using the formula given by Hutchinson,[7] which reads

$$\nu_{1\to 2}^{RR} = 5.2\sqrt{x[(\ln^2 x)+2]}(1-e^{-2x}) \quad [10^{-14}\mathrm{cm}^3/\mathrm{s}],$$

where $x = 4\cdot 13.6\,\mathrm{eV}/T_e$. This formula considers a Maxwellian electron distribution centered in the projectile system, and hence, it does not take into account the projectile velocity. In spite of this, if we consider $T_e = 10\,\mathrm{keV}$, $B = 3\,\mathrm{T}$, $E_\alpha = 3.5\,\mathrm{MeV}$, and only include the possibility of capturing one electron, we obtain a diffusion coefficient of approximately $1.8\times 10^{-4}\,\mathrm{m}^2/\mathrm{s}$, which is very close to the value obtained by Fussmann. This coefficient is very small when compared with the anomalous diffusion produced by other processes because the reaction rate for radiative recombination is very small in the core of a fusion reactor. In this work, we pay special attention to several other mechanisms, described by Eqs. (12) and (13), which significantly increase the diffusion coefficient in conditions relevant for the edge and SOL regions.

The basic definition of the diffusion coefficient given in Eq. (1) is valid, provided the displacement (Δl) is much smaller than the typical scale length of the density gradient. In a fusion reactor, the densities and temperatures of the plasma and neutral species will be nonuniform and have large gradients near the edge and pedestal. In addition, the width of the orbits of energetic particles will be large, especially for trapped particles. In this situation, calculating particle diffusion by solving a complicated transport equation, with nonuniform diffusion coefficients calculated using the equations given above, may not be appropriate. A better alternative is to perform particle simulations where the probability of charge changes by the processes indicated above is introduced via a Monte Carlo type random process. We developed a numerical code that follows the exact particle trajectories and calculates charge changes by assigning a probability proportional to the corresponding collision frequency of each process. The code runs on a graphic processor unit (GPU) and was tested by recovering exactly the same results as with Eq. (11) in the case of a uniform plasma (see Figs. 4 and 5). Classical (Coulomb) collisions are not included in the code.

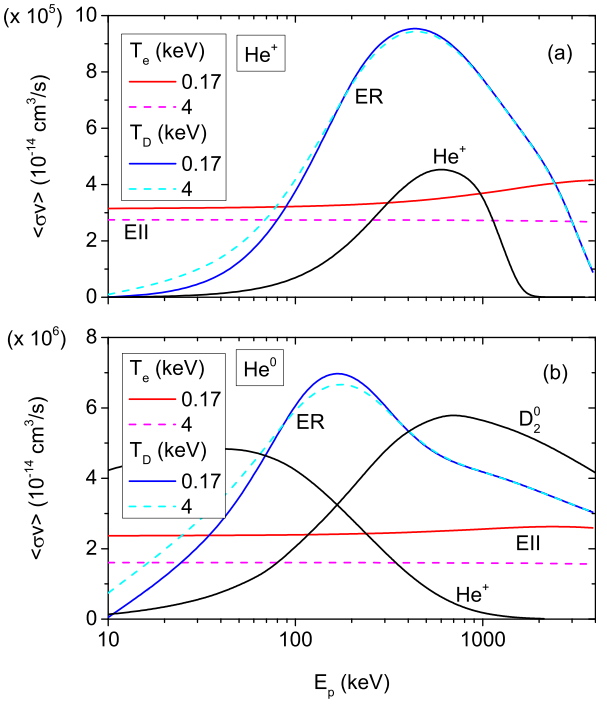

FIG. 3. Reaction rates employed for electron impact ionization (EII) and electron removal (ER: DII + CX) of alpha particles and thermal plasma species. In (a), we show the processes given by Eq. (13a) while in (b) those given by Eq. (13b).

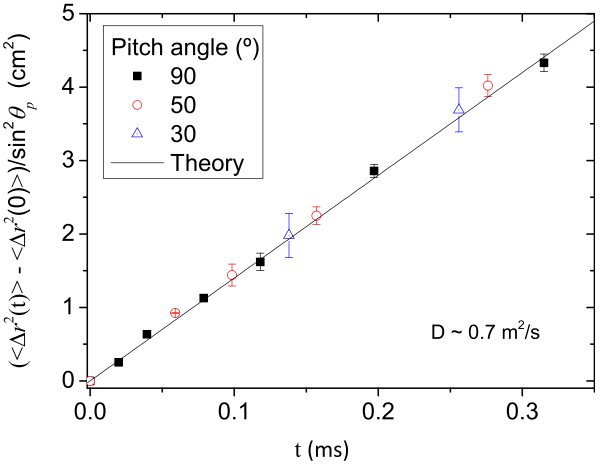

FIG. 4. Analytical and numerical results for the evolution of the variance, with pedestal parameters. Beams of particles with $E = 100\,\mathrm{keV}$ and different pitch is used. Analytical results for $\theta_p = 90°$ are included. The $\sin^2\theta_p$ dependence is clear. The neutralization channel is disabled.

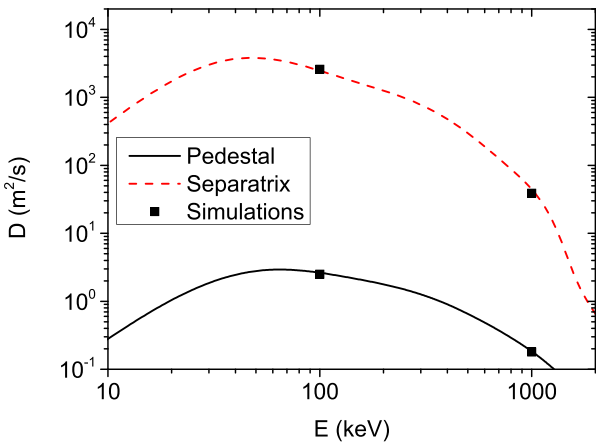

FIG. 5. Analytical diffusion coefficient for conditions (a) and (b) (see the text).

A. Uniform magnetic field, density and temperature profiles

To test the code, we followed the evolution of various beams of alpha particles, all with the same energy and different values of the pitch, θ_p. In this case, we have

$$\langle v_\perp^2 \rangle = (v \sin\theta_p)^2.$$

To compute the reaction frequency, we chose typical conditions for two plasma regions: (a) the pedestal and (b) the edge-SOL. For the pedestal, we assume: $T = 4\,\text{keV}$, $n_e = 0.98 \cdot 10^{14}\,\text{cm}^{-3}$, and $n_n = 6 \cdot 10^{10}\,\text{cm}^{-3}$. For the edge-SOL, we use: $T = 0.17\,\text{keV}$, $n_e = 4 \cdot 10^{13}\,\text{cm}^{-3}$, and $n_n = 7.3 \cdot 10^{11}\,\text{cm}^{-3}$. These are typical values obtained from the literature.[8,9]

The position of a particle is given by $\mathbf{r}_i(t) = x_i(t)\hat{x} + y_i(t)\hat{y}$, where "$i$" indicates the particles. To quantify the spreading of the beam, we introduce the variance, defined as

$$\langle \Delta r^2(t) \rangle = \frac{1}{N} \sum_{i=1}^{N} [r_i(t) - \bar{r}(t)]^2,$$

where N is the total number of particles and $\bar{\mathbf{r}}(t)$ is the position of the center of mass. The guiding center of the particles were initially distributed according to a Gaussian distribution with variance $\langle \Delta r^2(0) \rangle$. In a standard diffusion process, the variance should increase linearly with time. Using Eq. (1), we can write

$$\frac{\langle \Delta r^2(t) \rangle - \langle \Delta r^2(0) \rangle}{\sin^2\theta} = 2\,D\,t.$$

In Fig. 4, the full line was obtained using Eq. (4) with $\theta_p = \pi/2$ and the dots with our particle code, with the neutralization channel disabled and different values of θ_p. It can be seen that the agreement between both calculations is excellent and that the pitch dependence scales as expected. The linear increase in $\langle \Delta r^2 \rangle$ with time indicates that a standard diffusive process occurs. The diffusion coefficient, obtained from the slope of the full line, is $D = 0.7\,\text{m}^2/\text{s}$. In the remainder of this section, we will use $\sin\theta_p = 1$.

Figure 5 shows the diffusion coefficient as a function of the energy for the two sets of conditions indicated above. In this case, we allow the alpha particles to become neutralized and use Eq. (11) for the analytical calculation. The diffusion coefficient calculated with the pedestal's parameters shows a maximum at around 60 keV, with a value of approximately $3\,\text{m}^2/\text{s}$. For $E_\alpha = 100\,\text{keV}$ and the density and temperature corresponding to the pedestal (values used in Fig. 4), the diffusion coefficient results $D \simeq 2.5\,\text{m}^2/\text{s}$, instead of $0.7\,\text{m}^2/\text{s}$. This shows that including the possibility of neutralization produces a large increase in the diffusion coefficient, and that the values obtained can be larger than those resulting from other "anomalous" processes.

The diffusion coefficient for condition (b) has very large values, on the order of 10^2–$10^3\,\text{m}^2/\text{s}$. We show in Fig. 7 that this produces a rapid depletion of the alpha particles population in the edge-SOL region. Finally, we also include in this figure the results of our simulations (dots) to show the excellent agreement between both calculations.

B. Uniform magnetic field and non-uniform density and temperature profiles

The cases studied in Sec. IV A are not very realistic, but they were useful to get an idea of the importance of inelastic diffusion processes. In order to improve our description, in this section, we use a 1D model that includes nonuniform density and temperature profiles.

The electron density profile is assumed to be a hyperbolic tangent from the core to the separatrix, followed by an exponential decay from the separatrix to the wall. This profile is typically used in the literature.[10] We set $n_e = 10^{14}\,\text{cm}^{-3}$ in the core, $4 \cdot 10^{13}\,\text{cm}^{-3}$ at the separatrix, and $10^{13}\,\text{cm}^{-3}$ at the wall.[8] For the temperature, we use linear profiles, considering $T_e = 20\,\text{keV}$ at the center of the plasma ($x = 0$), 4 keV for the pedestal, 170 eV at the separatrix, and ~10 eV at the wall.[8,11]

For the neutral density, we used the same method as for the electron density but reversed: a hyperbolic tangent from wall to the separatrix and then an exponential decay into the plasma core. Near the wall, we set $n_n = 10^{12}\,\text{cm}^{-3}$ (Refs. 9 and 12), and inside the plasma, we match the values obtained by Afanasyev *et al.*[13] The magnetic field is uniform and equal to 5.3 T, and the pedestal is assumed to be at $x = 0.95$, the separatrix at $x = 1$, and the wall at $x = 1.025$.

Figure 6 shows the density and temperature profiles (right axis) and the diffusion coefficients obtained using Eq. (11), with $E_\alpha = 100\,\text{keV}$ and 1 MeV (left axis). The electron density and the temperature are normalized with their values at the center and the neutral density with its value at the wall. It is clear that very large diffusion coefficients can be obtained in the region between the pedestal and the separatrix.

Figure 7 shows the results of a simulation performed with 320 000 particles using our code. The curves were constructed from histograms that have a "box" size (Δx) equal to 0.00125 and the value of the "density" shown in the vertical axis was obtained by dividing the actual number of particles in a box, including all charge states, by the average number. The alpha particles, all with charge +2 and the same energy,

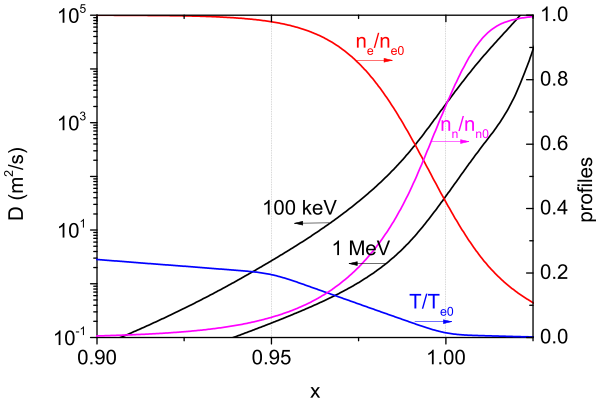

FIG. 6. Analytical diffusion coefficients (left scale) and profiles (right scale) for the 1D case studied ($T_{e0} = 20$ keV, $n_{e0} = 10^{14}$ cm^{-3} and $n_{n0} = 10^{12}$ cm^{-3}). The pedestal is at $x = 0.95$, the separatrix is at $x = 1$ and the wall is at x = 1.025. The region between the separatrix and the wall has very large values of the diffusion coefficient.

were initially loaded with the spatial distribution shown by the $t = 0$ (black) curve, and no particles were added after the simulation started (no sources). The initial alpha particles density profile was obtained by assuming that the distribution of guiding centers has an exponential decay[14] for $x \leq 1$, and is zero for $x > 1$. The rapid linear decrease around $x = 1$ is due to the random initial directions assumed for the velocities, which determine the actual position of the particles. The density and temperature profiles of the plasma and neutral species are those shown in Fig. 6. The energy is 100 keV in Fig. 7(a) and 1 MeV in Fig. 7(b).

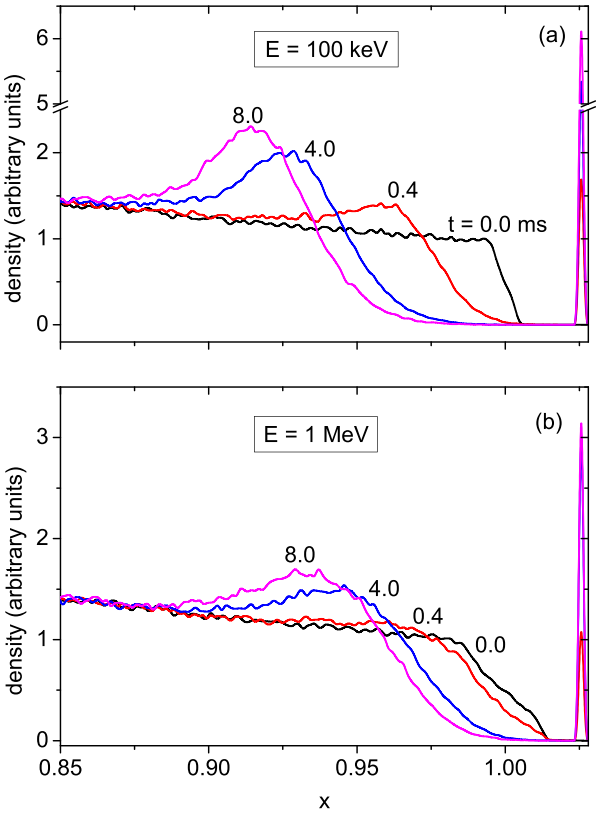

FIG. 7. Simulation of the evolution of the alpha particles density profile for the plasma and neutral density profiles shown in Fig. 6. Time (in ms) indicated on the curves. No source terms included.

It is clear that due to the large value of the diffusion coefficient in the region with $x > 0.95$, this region is rapidly depleted of alpha particles. Particles in this region have a high probability of becoming neutralized, and when this occurs, they rapidly move to the wall or return to the plasma, depending on the sign of their velocity. The peaks shown on the right side of the plots represent the neutral particles that hit the wall. The fraction of these particles is shown in Table I for both energies and different times.

Figures 7(a) and 7(b) also show that although the initial alpha particles density decreases with x, a large fraction of the particles located in the region $0.95 \lesssim x \lesssim 1$ actually move inwards (contrary to the density gradient). This produces a density peak that grows with time and moves inwards. The inward motion is due to the gradients in the plasma and neutral densities and can be qualitatively explained as follows. If an alpha particle with charge +2 captures an electron when it is in the outer (lager x) part of the orbit its guiding center jumps inwards a distance equal to the Larmor radius. If the electron capture occurs when it is in the inner (smaller x) part of the orbit the opposite occurs. Since the electrons are captured from the neutral population, and the neutral density increases with x, the probability of capturing an electron is larger on the outer part of the orbit and an average inward displacement results.

If an alpha particle with charge +1 losses an electron when it is on the inner (smaller x) part of the orbit its guiding center jumps inwards and the opposite occurs if the electron is lost on the outer part of the orbit. Since the electrons are lost mostly by impact with the plasma electrons and deuterons, and the plasma density decreases with x an average inward motion also occurs. When an alpha particle becomes neutralized, it has equal probabilities of moving inwards and outwards so the neutralization process does not produce a net flux. In others words, only the changes between charge states +2 and +1 contribute to the inward flux.

Figures 8(a) and 8(b) present additional information about this process by showing the evolution of a Gaussian alpha particles density profile (the initial charge of all the particles is +2). In both figures, the plasma and neutral density profiles are the same as in Fig. 7, but in Fig. 8(a), the neutralization channel has been switched off. It can be clearly seen that in addition to spreading (diffusion), the density peak moves inwards and the evolution is basically the same with, or without, the possibility of neutralization.

Note that the alpha particles density profiles shown in Figs. 7 and 8 were obtained without including source terms and other diffusion mechanisms, such as classical collisions and turbulence. In an actual situation, with source terms inside the plasma, the stationary profiles will result from a

TABLE I. Percentage (%) of particles that reach the wall in Fig. 7. The total number of particles is 320 000.

Time (ms)	$E_\alpha = 100$ keV	$E_\alpha = 1$ MeV
0.4	1.7	0.8
4.0	3.6	2.2
8.0	4.2	2.3

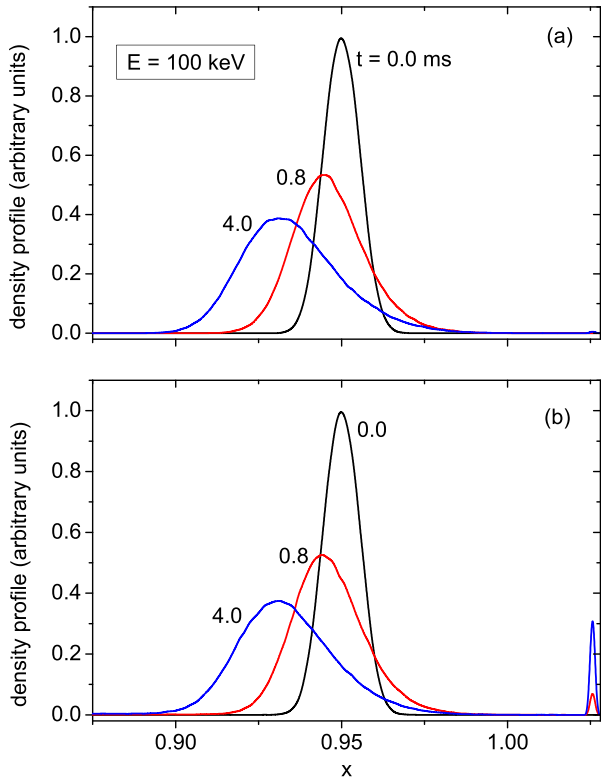

FIG. 8. Simulation of the evolution of a Gaussian profile of alpha particles for the plasma and neutral density profiles shown in Fig. 6. Time (in ms) indicated on the curves. No source terms included.

balance between the source term and diffusion produced by different processes.

V. SUMMARY AND CONCLUSIONS

We presented analytical calculations and particle simulations that show that charge changing processes can significantly increase the diffusion of alpha particles in the pedestal-edge-SOL regions. To the best of our knowledge, this is the first study that presents clear evidence of the importance of these processes. The only existing study on this topic[1] considered a different situation and concluded that alpha particle diffusion was not affected by charge changing processes. We employed a simple 1D model and only included the interaction of the alpha particles with the plasma species, He^+ and neutral deuterium (both atomic and molecular) and helium. The numerical code calculates the exact alpha particles trajectories and introduces the probability of charge changing events via a Monte Carlo type method, where the probability of each process is taken proportional to the corresponding collision frequency. The cross sections of these processes were obtained from the existing databases but it is clear that more, and more accurate, atomic data are needed. The code runs on a GPU, thus allowing calculations with a large number of particles in a short time using modest computational resources.

The main conclusion of this study is that once the alpha particles reach the pedestal region, the mechanism considered above becomes important and calculations of the alpha particle flux to the wall and divertor should include charge changing processes. It is also important to note that due to the inward flux, the alpha particle density should be very low near the separatrix, which is the region where the confinement can be significantly affected by the toroidal field ripple and the perturbations produced by ELM control coils. In future studies, we will use a more realistic 2D toroidal equilibrium and include the interaction with partially ionized impurities, such as Be or W, if the atomic data are available. Although the effect of charge changes on the diffusion of trapped particles has not been studied in detail, the presence of trapped alpha particles with large banana widths could substantially increase the diffusion coefficient. Since the results are very sensitive to the value of the neutral density, more accurate experimental information and predictions regarding the density profiles of neutral particles and partially ionized impurities will be needed to obtain results that can be reliable applied to future reactors.

ACKNOWLEDGMENTS

This work was supported by the Comisión Nacional de Energía Atómica, CNEA (Controlled Nuclear Fusion Program) and Universidad Nacional de Cuyo. C.F.C. acknowledges the support of the Consejo Nacional de Investigaciones Científicas y Técnicas (CONICET), Argentina.

[1]G. Fussmann, Contrib. Plasma Phys. **37**, 363 (1997).
[2]T. Kurki-Suonio, O. Asunta, T. Hellsten, V. Hynönen, T. Johnson, T. Koskela, J. Lönnroth, V. Parail, M. Roccella, G. Saibene, A. Salmi, and S. Sipilä, Nucl. Fusion **49**, 095001 (2009).
[3]A. Snicker, S. Sipilä, and T. Kurki-Suonio, Nucl. Fusion **52**, 094011 (2012).
[4]*Atomic and Molecular Processes in Fusion Edge Plasmas*, edited by R. K. Janev (Springer US, Boston, MA, 1995).
[5]See https://www-amdis.iaea.org/ALADDIN/ for IAEA AMDIS ALADDIN Database.
[6]C. F. Barnett, "Atomic data for fusion," Technical Report No. ORNL - 6086/V1, Oak Ridge National Laboratory, 1990.
[7]I. H. Hutchinson, *Principles of Plasma Diagnostics* (Cambridge University Press, Cambridge, 2002).
[8]A. Kukushkin, H. Pacher, G. Pacher, G. Janeschitz, D. Coster, A. Loarte, and D. Reiter, Nucl. Fusion **43**, 716 (2003).
[9]A. Kukushkin, H. Pacher, V. Kotov, D. Reiter, D. Coster, and G. Pacher, Nucl. Fusion **45**, 608 (2005).
[10]M. A. Mahdavi, R. Maingi, R. J. Groebner, A. W. Leonard, T. H. Osborne, and G. Porter, Phys. Plasmas **10**, 3984 (2003).
[11]A. R. Polevoi, S. Medvedev, V. Mukhovatov, A. Kukushkin, Y. Murakami, M. Shimada, and A. Ivanov, J. Plasma Fusion Res. Ser. **5**, 82 (2002), available at http://www.jspf.or.jp/JPFRS/index_vol5.html.
[12]V. Kotov, D. Reiter, and A. S. Kukushkin, "Numerical study of the ITER divertor plasma with the B2-EIRENE code package," Technical Report No. Jül-4257, 2007, available online at http://www.eirene.de/html/relevant_reports.html and http://www.eirene.de/kotov_solps42_report.pdf.
[13]V. I. Afanasyev, F. V. Chernyshev, A. I. Kislyakov, S. S. Kozlovski, B. V. Lyublin, M. I. Mironov, A. D. Melnik, V. G. Nesenevich, M. P. Petrov, and S. Y. Petrov, Nucl. Instrum. Methods Phys. Res., Sect. A **621**, 456 (2010).
[14]V. I. Afanasyev, M. I. Mironov, V. G. Nesenevich, M. P. Petrov, and S. Y. Petrov, Plasma Phys. Controlled Fusion **55**, 045008 (2013).